Fast Track Communications

IOP Publishing

Smart Materials and Structures

Smart Mater. Struct. **23** (2014) 092001 (8pp)

doi:10.1088/0964-1726/23/9/092001

Fast Track Communications

Dielectric loss against piezoelectric power harvesting

Junrui Liang[1,4], Henry Shu-Hung Chung[2] and Wei-Hsin Liao[3]

[1] School of Information Science and Technology, ShanghaiTech University, Shanghai, People's Republic of China

[2] Centre for Smart Energy Conversion and Utilization Research, City University of Hong Kong, Hong Kong, People's Republic of China

[3] Department of Mechanical and Automation Engineering, The Chinese University of Hong Kong, Hong Kong, People's Republic of China

E-mail: liangjr@shanghaitech.edu.cn

Received 27 March 2014, revised 22 May 2014
Accepted for publication 13 June 2014
Published 24 July 2014

Abstract

Piezoelectricity is one of the most popular electromechanical transduction mechanisms for constructing kinetic energy harvesting systems. When a standard energy harvesting (SEH) interface circuit, i.e., bridge rectifier plus filter capacitor, is utilized for collecting piezoelectric power, the previous literature showed that the power conversion can be well predicted without much consideration for the effect of dielectric loss. Yet, as the conversion power gets higher by adopting power-boosting interface circuits, such as synchronized switch harvesting on inductor (SSHI), the neglect of dielectric loss might give rise to deviation in harvested power estimation. Given the continuous progress on power-boosting interface circuits, the role of dielectric loss in practical piezoelectric energy harvesting (PEH) systems should receive attention with better evaluation. Based on the integrated equivalent impedance network model, this fast track communication provides a comprehensive study on the susceptibility of harvested power in PEH systems under different conditions. It shows that, dielectric loss always counteracts piezoelectric power harvesting by causing charge leakage across piezoelectric capacitance. In particular, taking corresponding ideal lossless cases as references, the counteractive effect might be aggravated under one of the five conditions: larger dielectric loss tangent, lower vibration frequency, further away from resonance, weaker electromechanical coupling, or using power-boosting interface circuit. These relationships are valuable for the study of PEH systems, as they not only help explain the role of dielectric loss in piezoelectric power harvesting, but also add complementary insights for material, structure, excitation, and circuit considerations towards holistic evaluation and design for practical PEH systems.

Keywords: energy harvesting, piezoelectric materials, dielectric loss, switching interface circuits, impedance modeling

1. Introduction

The interest of kinetic energy harvesting using piezoelectric materials has endured for more than a decade [1] and has become even more intensive in recent times [2, 3] given the growing trends of ubiquitous wireless sensor networks and wearable electronics. Innovative designs on both mechanical structures and energy harvesting interface circuits have been proposed and extensively studied for enhancing the bandwidth and power density of piezoelectric energy harvesting (PEH) systems [2, 3]. In most of the early studies, in particular those considering standard energy harvesting (SEH)

[4] Author to whom any correspondence should be addressed.

interface circuit [4] or resistive load [5], neglecting the effect of dielectric loss (even it is one of the important parasitic features of piezoelectric materials) seemed to draw little derivation on power estimation. However, when a power-boosting circuit, such as synchronized switch harvesting on inductor (SSHI), is connected, Liang and Liao found that some experimental observation and power overestimation were unable to be properly explained based on the lossless assumption [6]. As it was reported that the influence of dielectric loss increases intensively under high-power operation [7], the error in power estimation might become even bigger for some recently reported interface circuits, which aim to further increase the power density of piezoelectric materials [8, 9]. Given the popular usage of synchronized switch power-boosting interface circuit for piezoelectric devices [10–12], as well as that some commonly used piezoelectric materials might have considerable dielectric loss, e.g., polyvinylidene fluoride (PVDF) [13], the role of dielectric loss in practical PEH systems is not trivial and should receive comprehensive consideration, so as to provide a proper description of system dynamics as well as an accurate estimation of harvested power in PEH systems.

Integrated analysis is emphasized in this paper for finding the role of dielectric loss in practical PEH systems. The mechanical part of practical PEH systems is usually parameter distributed structure, while the electrical part is nonlinear harvesting interface circuit. Advanced mathematical models have been well developed for describing the dynamic behaviors of either side; yet, model integration for the both parts is troublesome [14]. In most existing literature emphasizing the design or analysis of mechanical structure, their harvesting circuits were simply taken as an equivalent resistor [2]; In that focus on the design or performance of the harvesting circuit, the mechanical behavior was simply regarded as an equivalent current source [3]. Simplified models may not be able to provide accurate integrated analysis for a holistic PEH system. In contrast to those modeling methodologies, Shu *et al* proposed an integrated analysis for PEH systems based on differential equations and energy balance [15–17]. And later Liang and Liao developed the equivalent impedance network model based on fundamental harmonic analysis [18]. The impedance method takes both mechanical and electrical sides into more balanced consideration, so that their overall dynamics can be appropriately described. The equivalent impedance network model is able to be further extended by considering the effect of other constitutive elements, e.g., the dielectric leakage. Because of its easy extension feature and innate convenience on power analysis, the equivalent impedance network model is taken as the theoretical base of this paper for investigating the role of dielectric loss in practical PEH systems.

2. Theory

Figure 1 shows the equivalent impedance network of a linear PEH system under one of its vibration modes, while figure 2 shows the corresponding equivalent mechanical schematics. The two figures are presented in purely electrical or mechanical styles, but they have the same underlying mathematics [18]. $v_{eq}(t)$ and $i_{eq}(t)$ in figure 1 are equivalent voltage and current. They correspond to the excitation force $f(t)$ and vibration velocity $\dot{x}(t)$ in figure 2 with the following relations

$$v_{eq}(t) = \frac{f(t)}{\alpha_e}, \qquad i_{eq}(t) = \alpha_e \dot{x}(t), \tag{1}$$

where α_e is the force–voltage factor of piezoelectric element. In figure 1, L, R, C, and C_{sc} in series form the resonant path, whose resonance frequency corresponds to one of the vibration modes of the piezoelectric structure. These four components correspond to the equivalent mass M, damping coefficient D, stiffness of substrate structure K, and stiffness of piezoelectric element under short circuit condition K_{sc}. Yet, because of the voltage versus force and current versus velocity electromechanical analogy, the series connection in the electrical domain is turned into a parallel one in the mechanical domain, as shown in figure 2. The relations of these components in the electromechanical analogy are given as follows

$$L = \frac{M}{\alpha_e^2}; \qquad R = \frac{D}{\alpha_e^2}; \qquad C = \frac{\alpha_e^2}{K}; \qquad C_{sc} = \frac{\alpha_e^2}{K_{sc}}. \tag{2}$$

C_e, R_h, and R_d in figure 1 are the electrically induced capacitance, harvesting component, and dissipative component [18]. These three equivalent components are derived from the combination of the clamped capacitance C_p and its shunt harvesting interface circuit. The total power consumed by R_h and R_d equals to the power extracted from piezoelectric structure. Such power extraction induces an additional damping effect to the vibrating system. The counterparts of C_e, R_h, and R_d in the mechanical domain are denoted as K_e, D_h, and D_d respectively, as shown in figure 2. They are linked with the following relations

$$K_e = \frac{\alpha_e^2}{C_e}; \qquad D_h = \alpha_e^2 R_h; \qquad D_d = \alpha_e^2 R_d. \tag{3}$$

The roles of these electrically induced components can be distinguished and quantified through energy flow analysis [19]. The available ranges for these electrically induced components are different under different adopted interface circuits; within the constraint, which is set by a specific circuit, the values of these components are tunable by changing the non-dimensional rectified voltage $\tilde{V}_{rect}$. The variability of these equivalent components and their dependence on $\tilde{V}_{rect}$ are illustrated with arrows and dot line linkages in figures 1 and 2.

Besides the aforementioned components, which were discussed in detail by Liang and Liao [18], a leakage resistance R_p is added in this study for the purpose of discussing the function of dielectric loss in practical piezoelectric materials. This complement to the previous equivalent impedance model enables better explanation of some experimentally observed phenomena [6] and makes the power estimation of practical PEH systems more accurate. D_p is the counterpart of R_p in the mechanical domain, as shown in

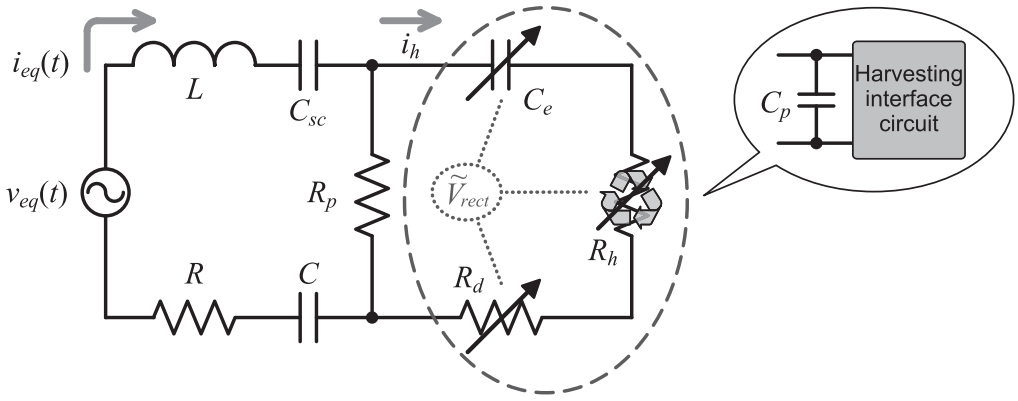

Figure 1. Equivalent impedance network of a PEH system.

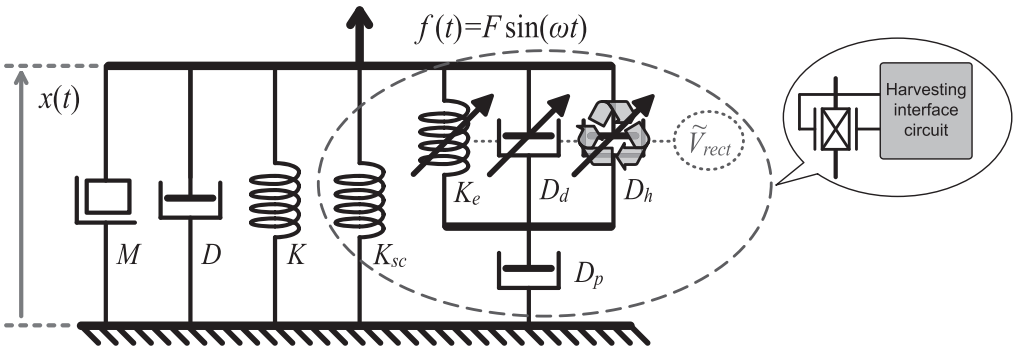

Figure 2. Equivalent mechanical schematics of a PEH system.

figure 2. R_p and D_p are correlated with the following relation

$$D_p = \alpha_e^2 R_p \,. \tag{4}$$

Given the parallel connection between R_p and the C_e–R_d–R_h path in electrical domain, corresponding D_p in mechanical domain is equivalent to a dash pot suspending (in series connection) the three electrically tunable components K_e, D_d, and D_h, as illustrated in figure 2.

In general, as shown in figure 2, the installation of piezoelectric insert and its shunt harvesting interface circuit introduces an additional dynamic network, which is composed of K_{sc}, K_e, D_d, D_h, and D_p, to the vibrating system. Compared to the extensively referred general harvester model proposed by Williams and Yates [20], where the effect of energy harvester is regarded as only an equivalent dash pot, this model is able to describe the dynamic behavior of practical PEH systems more exactly. In addition, the understanding on the holistic context makes it possible to carry out parametric studies to reveal the roles of different constitutive elements, including the dielectric loss equivalence D_p.

As observed from figure 1, if the piezoelectric materials are lossless, i.e., $R_p = \infty$, i_h, the current flowing through R_h, equals to i_{eq}. Under harmonic excitation, the ideal harvested power by assuming lossless piezoelectric materials is given by

$$P_{h,lossless} = \frac{I_{eq}^2 R_h}{2} = \frac{V_{eq}^2 R_h}{2} \left| \frac{1}{Z_m + Z_e} \right|^2 , \tag{5}$$

where I_{eq} and V_{eq} are the magnitudes of $i_{eq}(t)$ and $v_{eq}(t)$, respectively. Z_m and Z_e are sums of equivalent impedances in mechanical part and electrical part (without R_p), respectively, i.e.,

$$\begin{aligned} Z_m &= R + j\omega L + \frac{1}{j\omega C} + \frac{1}{j\omega C_{sc}} \\ &= \frac{1}{\alpha_e^2}\left[D + j\left(\omega M - \frac{K + K_{sc}}{\omega} \right) \right], \end{aligned} \tag{6}$$

$$Z_e = R_h + R_d + \frac{1}{j\omega C_e} , \tag{7}$$

where ω is the vibration frequency of the PEH system. When dielectric loss is considerable, the lossless estimation is no longer valid. In this case, R_p is finite, the harvested power considering dielectric loss therefore can be derived as follows

$$\begin{aligned} P_{h,lossy} &= \frac{I_{eq}^2 R_h}{2} \left| \frac{R_p}{R_p + Z_e} \right|^2 \\ &= \frac{V_{eq}^2 R_h}{2} \left| \frac{R_p}{Z_m R_p + Z_m Z_e + Z_e R_p} \right|^2 . \end{aligned} \tag{8}$$

Table 1. Influential factors of relative power ratio A_F and corresponding tuning methods in validating tests.

Related portion	Influential factor	Tuning variable	Tuning method
material	$\tan\delta$	$\tan\delta$	connecting different shunt resistor $R_{p,ex}$
	$\widetilde{Z}_m$	α_e	applying constant F or $\dot{X}$ excitations
structure		$\lvert\omega-\omega_{sc}\rvert$	changing excitation frequency
excitation	ω	ω	
circuit	$\widetilde{Z}_e$	$\widetilde{Z}_e$	using different harvesting circuits

Dividing (8) by (5) gives the *relative power ratio* for evaluating the effect of dielectric loss towards harvested power. Yet, this factor depends on excitation condition. When the system is excited under constant velocity magnitude, i.e., constant $\dot{X}$, since $I_{eq}=\alpha_e\dot{X}$, the relative power ratio can be obtained as follows

$$A_{\dot{X}}=\left.\frac{P_{h,lossy}}{P_{h,lossless}}\right|_{\text{const. }\dot{X}}=\frac{1}{\left|1+\tan\delta\left(\frac{\omega_t}{\omega}\right)\tilde{Z}_e\right|^2}, \tag{9}$$

where

$$\tan\delta=\frac{1}{\omega_t C_p R_p} \tag{10}$$

is dielectric loss tangent of piezoelectric material, which is determined under the testing frequency ω_t. ω_t is usually selected to be 1 kHz according to specifications from most piezoelectric material manufacturers [21, 22].

$$\tilde{Z}_e=Z_e\omega C_p \tag{11}$$

is a non-dimensional factor isolating the contribution of harvesting interface circuit [18]. If the system is excited by a force with constant magnitude, i.e., constant F, since $V_{eq}=F/\alpha_e$, dividing (8) by (5), the relative power ratio becomes

$$A_F=\left.\frac{P_{h,lossy}}{P_{h,lossless}}\right|_{\text{const. }F}=\frac{1}{\left|1+\tan\delta\left(\frac{\omega_t}{\omega}\right)\left(\tilde{Z}_m\parallel\tilde{Z}_e\right)\right|^2}, \tag{12}$$

where

$$\tilde{Z}_m=Z_m\omega C_p \tag{13}$$

is the non-dimensional factor of the equivalent mechanical part impedance. $\tilde{Z}_m$ includes information about mechanical dynamics, as given by (6), and also that about electromechanical coupling. For instance, under quasistatic operation ($\omega\to 0$), we can have

$$\left|\tilde{Z}_m\right|_{\omega\to 0}=\frac{(K+K_{sc})C_p}{\alpha_e^2}=\frac{1-k^2}{k^2}, \tag{14}$$

where k^2 is the coupling coefficient of the piezoelectric structure.

In (9) and (12), $\tan\delta$, ω_t/ω, Re $[\tilde{Z}_m]$, and Re $[\tilde{Z}_e]$ are all above zero, making both $A_{\dot{X}}$ and A_F smaller than one. Therefore, harvested power under dielectrically lossy condition is smaller than that under lossless condition. In another word, *dielectric loss always counteracts piezoelectric power harvesting*.

More information about the counteractive effect resulting from dielectric loss can be dug out by further investigating (9) and (12). From (9), the increase of $\tan\delta$, $1/\omega$, or Re $[\tilde{Z}_e]$ reduces $A_{\dot{X}}$, i.e., aggravates the counteractive effect. As for A_F, it approximates $A_{\dot{X}}$ when $|\tilde{Z}_m|\gg|\tilde{Z}_e|$. From (6), such condition is attained when electromechanical coupling is weak, i.e., $\alpha_e\to 0$, or vibration is far away from resonance, i.e., $\omega\ll\omega_{sc}$ or $\omega\gg\omega_{sc}$, where

$$\omega_{sc}=\sqrt{\frac{K+K_{sc}}{M}} \tag{15}$$

is the resonant frequency under short circuit condition. When electromechanical coupling is considerable and, at the same time, ω approaches ω_{sc}, the magnitude of $\tilde{Z}_m\|\tilde{Z}_e$ becomes smaller than that of $\tilde{Z}_e$,[5] making

$$A_{\dot{X}}<A_F<1. \tag{16}$$

Since $A_{\dot{X}}$ can be taken as a special case of A_F, where backward coupling is so weak that extracting energy from the PEH system does not affect its vibration, A_F generalizes the counteractive role of dielectric loss in a holistic context. In addition, given that A_F is a function of $\tan\delta$, ω, $\tilde{Z}_m$, and $\tilde{Z}_e$, then generally speaking, the intensity of such counteractive effect is related to material, structure, excitation, and circuit portions of a PEH system. The correspondences are summarized in the first two columns of table 1.

3. Experimental validation

Experiments are carried out on a cantilevered PEH system, whose configuration and dimensions are illustrated in figure 3, in order to validate the proposed theory according to the practical power harvesting under different $\tan\delta$, ω, $\tilde{Z}_m$, and $\tilde{Z}_e$. Output impedance of the piezoelectric structure in use is measured with an impedance analyzer (4294A, Agilent), as shown by the discrete marks in figure 4(a). Assuming lossless

[5] Strictly speaking, such a relation is attained when $\tilde{Z}_e$ is approximately real numbers, i.e., $\angle\tilde{Z}_e\approx 0$. The real part of $\tilde{Z}_e$ is more dominated when a power-boosting interface circuit is adopted [18].

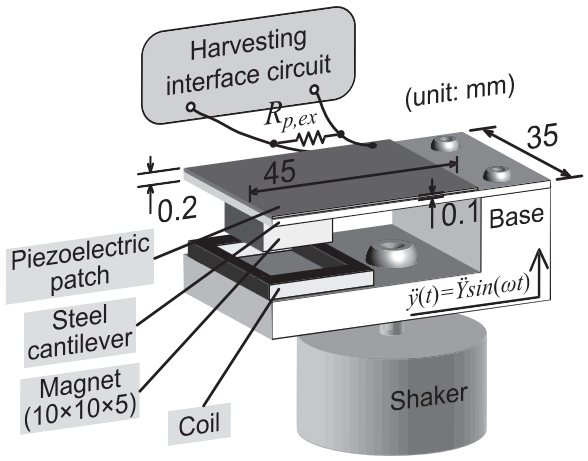

Figure 3. Experimental setup.

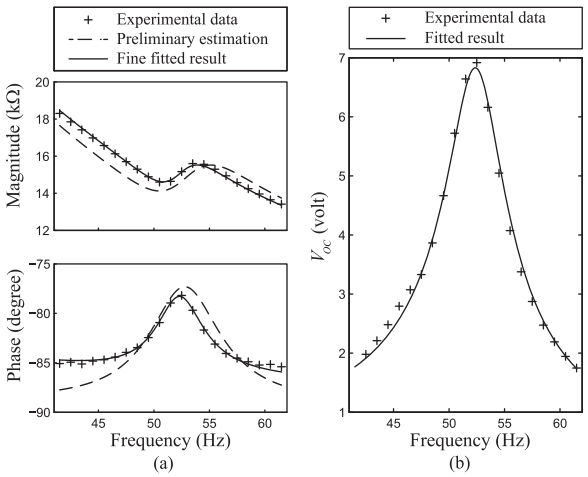

Figure 4. Parametric identification by fitting the measured data. (a) Impedance data. (b) Open circuit voltage.

condition, i.e., without considering R_p, at the beginning, the values of R, L, $C \parallel C_{sc}$, and C_p are preliminarily estimated based on the experimental data set. The preliminary estimation result is presented by dashed curves in figure 4(a). Taking these estimated values as the initial condition and assigning initial R_p as 1 MΩ, the values of R, L, $C \parallel C_{sc}$, C_p, and R_p are finely tuned by minimizing the error between the measured and fitted results. The final values of these parameters are listed in table 2; the finely fitted result is shown by solid curves in figure 4(a). To obtain the force-voltage factor α_e, more information is needed by fitting the open circuit voltage under constant force magnitude (proportional to acceleration here) excitation, as shown in figure 4(b). The estimated value of α_e is also listed in table 2.

Within the aforementioned four factors, which might influence the counteractive effect of dielectric loss, $\tan\delta$, ω, and $\tilde{Z}_e$ can be regarded as independent variables; the influence of $\tilde{Z}_m$ can be separately embodied by two independent variables: $|\omega - \omega_{sc}|$ indicating the frequency difference from resonance and α_e representing the electromechanical coupling. Therefore there are, in total, five independent variables,

Table 2. Identified parameters.

Parameter	Value
R	111.94 kΩ
L	3.44 kH
$C \parallel C_{sc}$	2.70 nF
C_p	199.73 nF
$R_{p,in}$	217.79 kΩ
α_e	0.0015 N/V
f_{sc}	52.14 Hz

which might affect A_F, to be investigated, as listed in the third column of table 1.

In experiments, dielectric loss tangent $\tan\delta$ is changed by connecting additional shunt resistor $R_{p,ex}$ across the piezoelectric element, as illustrated in figure 3. Since $\tan\delta$ is a function of R_p according to (10), by connecting $R_{p,ex}$, effective leakage resistance becomes $R_p = R_{p,in} \| R_{p,ex}$, where $R_{p,in}$ is inherent dielectric leakage resistance listed in table 2. As for α_e, theoretically, it is fixed once the piezoelectric material was made. Yet, given that $A_{\dot{X}}$ can be taken as a special case of A_F, where $\alpha_e = 0$, we can obtain the results under two discrete coupling conditions ($\alpha_e = 0$ and 0.0015 N/V, the factor of piezoelectric material in use, as listed in table 2) for comparative study. As a base acceleration $\ddot{y}$ yields proportional equivalent inertial force $-M\ddot{y}$ at the equivalent mass of the cantilever, the constant F and constant $\dot{X}$ conditions are realized by taking reference to the base acceleration measured by an accelerometer, and the relative velocity measured by an electromagnetic sensor respectively. Given a fixed piezoelectric structure used in experiment, ω_{sc} is constant. Vibration frequency ω and its difference to the resonant frequency, i.e., $|\omega - \omega_{sc}|$, can be simultaneously adjusted by tuning the frequency of shaker excitation signal. Circuit factor $\tilde{Z}_e$ depends on the selected interface circuit and non-dimensional rectified voltage $\tilde{V}_{rect}$. Power generation using different harvesting interface circuits, including standard energy harvesting (SEH) and two power-boosting interface circuits, i.e., parallel synchronized switch harvesting on inductor (P-SSHI) and series SSHI (S-SSHI), are investigated in experiments. Corresponding expressions of $\tilde{Z}_e$ in the three cases were given in the early study [18]. The tuning methods in the validating experiments are summarized in the fourth column of table 1.

According to the aforementioned four tuning methods, four groups of experiments are carried out to produce different testing conditions and to observe the harvested power under such conditions. In each experiment, results are obtained by varying two conditions, while the other two are fixed. Corresponding testing conditions in the four groups of experiments are summarized in table 3; while the results are shown in figures 5–8. Theoretical predictions show very good agreement with experimental results.

Under constant $\dot{X}$ excitation, where mechanical dynamics is excluded, it can be observed from figure 5 that frequency variation does not influence the harvested power much. On the other hand, from figure 6, the level of dielectric loss, in terms

Table 3. Testing conditions in four groups of experiments.

Testing condition	Exp #1	Exp #2	Exp #3	Exp #4
Excitation (in rms)	$\dot{X} = 0.30$ ms^{-1}		$\ddot{Y}_{ex} = 10$ ms^{-2}	
Shunt resistor $R_{p,ex}$	∞	100, 200, & ∞ kΩ	∞	100, 200, & ∞ kΩ
Frequency $f = \omega/(2\pi)$	50, 53, & 56 Hz	53 Hz	50, 53, & 56 Hz	53 Hz
Harvesting circuit	SEH, P-SSHI, & S-SSHI ($\gamma = -0.66$ in SSHI)			

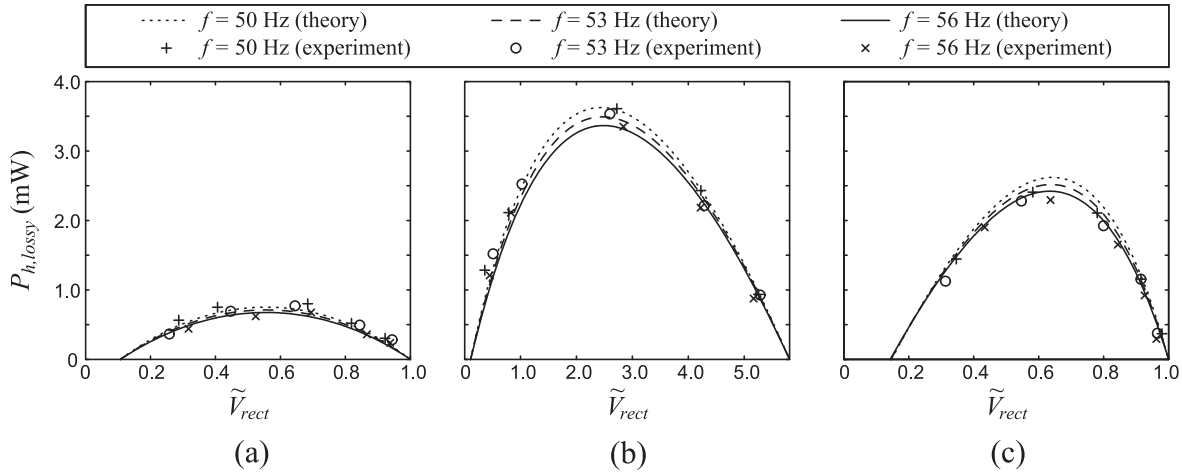

Figure 5. Results in experiment #1 (constant $\dot{X}$ and infinite $R_{p,ex}$). (a) SEH. (b) P-SSHI. (c) S-SSHI.

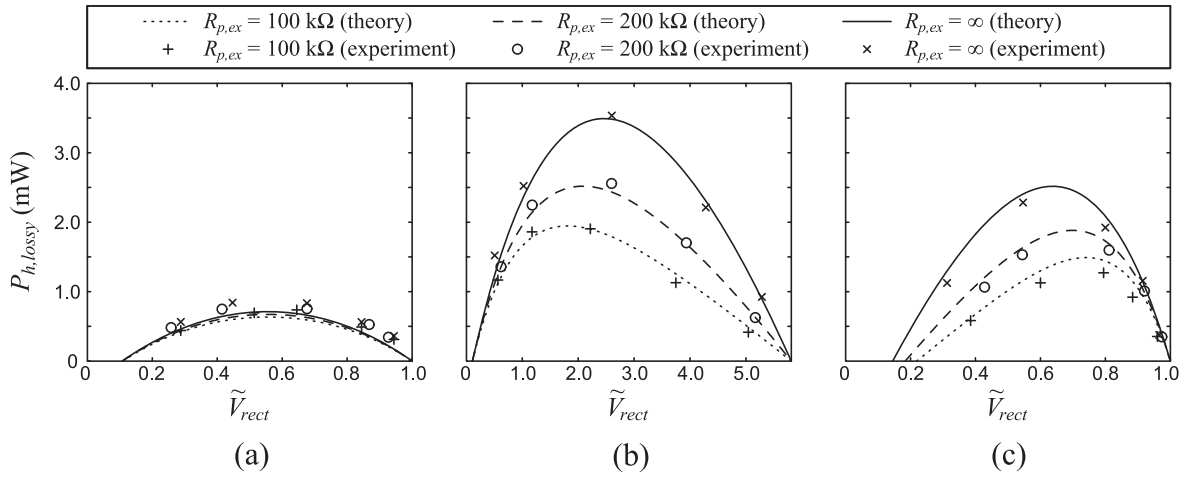

Figure 6. Results in experiment #2 (constant $\dot{X}$ and f). (a) SEH. (b) P-SSHI. (c) S-SSHI.

of R_p, has a different influence on the harvested power when different power-boosting interface circuits, which associate with different $\tilde{Z}_e$ magnitudes, are used. In SEH, the change of R_p does not make a significant difference, as shown in figure 6(a); yet, in P- and S-SSHI, the decrease of R_p makes the harvested power drop a lot, as shown in figures 6(b) and (c).

When the PEH system is excited under constant $\ddot{Y}_{ex}$, or equivalently constant inertial force magnitude, harvested power is sensitive to the difference between excitation and resonance frequency, regardless of harvesting interface circuits used, as shown in figure 7. Maximum harvested power is obtained around the resonant frequency, 52.14 Hz in this case. Figure 8 shows similar trend as figure 6, even they are obtained under different excitation conditions. In general, neglecting the effect of dielectric loss does not bring much error for power estimation in the SEH case; yet, might introduce large discrepancy if power-boosting interface circuits, such as P- and S-SSHI are used.

4. Discussion

Given the effectiveness of the equivalent impedance network model in predicting the harvested power under different

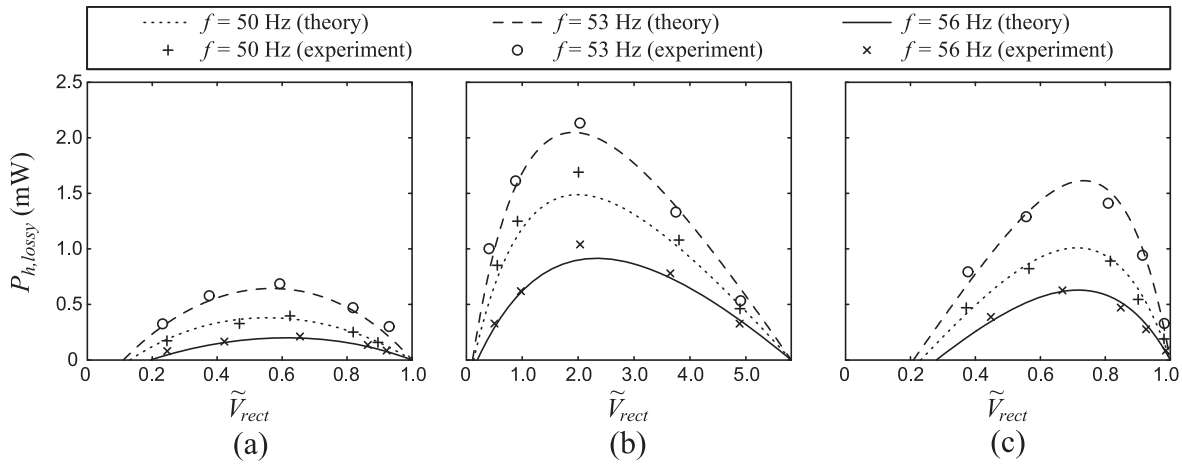

Figure 7. Results in experiment #3 (constant $\ddot{Y}_{ex}$ and infinite $R_{p,ex}$). (a) SEH. (b) P-SSHI. (c) S-SSHI.

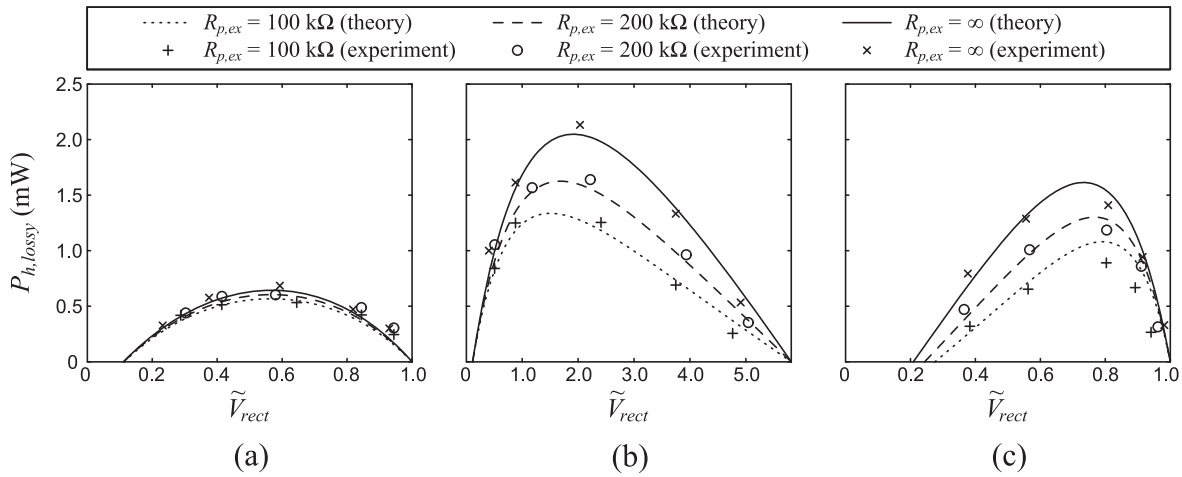

Figure 8. Results in experiment #4 (constant $\ddot{Y}_{ex}$ and f). (a) SEH. (b) P-SSHI. (c) S-SSHI.

testing conditions, the harvested power under practical lossy condition can be theoretically compared with that under ideal lossless condition, in terms of relative power ratio, which was defined in (9) and (12). Without connecting additional shunt resistor $R_{p,ex}$, figure 9 shows such a ratio under different frequencies, excitation conditions, and circuit conditions[6]; under 53 Hz vibration, figure 10 shows this relative power ratio under different dielectric losses, excitation conditions, and circuit conditions.

It can be seen from figures 9 and 10 that, all relative power ratios A are below one, which confirms the counteractive effect of dielectric loss against piezoelectric power harvesting. Moreover, five additional features corresponding to the five tuning variables listed in table 1 can be observed from the curves' trend in two figures. 1) From figure 10, the smaller R_p, i.e., larger dielectric loss tangent $\tan\delta$, the smaller relative power ratio A, i.e., less harvested power compared to the ideal lossless case. 2) From figures 9 and 10, comparing the ratios under constant force and constant velocity excitations, i.e., A_F and $A_{\dot{X}}$, with each interface circuit, $A_F > A_{\dot{X}}$ in general. Since constant force magnitude excitation represents larger α_e condition, relative power ratio A is lower with smaller α_e. 3) From figure 9, A_F becomes smaller and approaches $A_{\dot{X}}$ when the vibration is further away from resonance, in particular, for the SSHI cases. 4) From figure 9, without considering the effect of mechanical dynamics, $A_{\dot{X}}$ is smaller at lower vibration frequency. 5) From figures 9 and 10, the circuit factor towards the degradation of relative power ratio A is significant, no matter under constant $\dot{X}$ or F excitations. The magnitude of $\tilde{Z}_e$, whose real part corresponds to electrically induced damping effect, is significantly increased by using power-boosting interface circuits, such as P- and S-SSHI [18]. Recalling the order of harvesting capabilities of the three investigated circuits (SEH < S-SSHI < P-SSHI [23]), and observing the curves' level in figures 9 and 10, the counteractive effect of dielectric loss against power harvesting is aggravated when harvesting interface circuit with higher harvesting capability is used. Among the five factors, roughly speaking, the loss tangent and circuit factor have a bigger influence on the relative power ratio; while the other three factors, i.e., frequency from resonance, coupling factor, and vibration frequency, have a moderate influence.

[6] The peak harvested power obtained at optimum $\tilde{V}_{rect}$ by each harvesting interface circuit is regarded as the harvesting capability of the corresponding circuit.

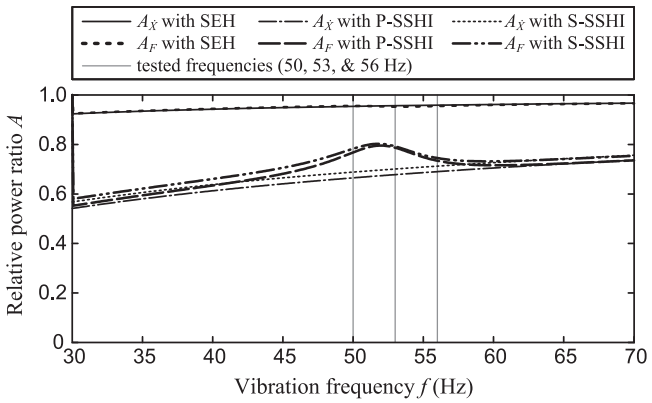

Figure 9. Relative power ratio under different frequencies, excitation conditions, and circuit conditions ($R_{p,ex} = \infty$).

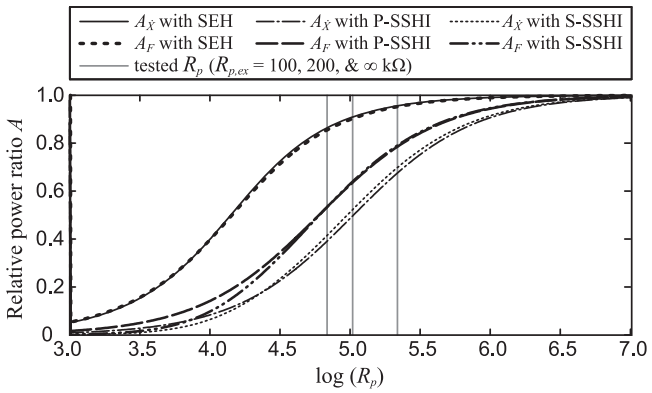

Figure 10. Relative power ratio under different dielectric losses, excitation conditions, and circuit conditions (f = 53 Hz).

5. Conclusion

The role of dielectric loss in practical piezoelectric energy harvesting (PEH) systems was investigated in this study. The intuitive conclusion that dielectric loss always counteracts piezoelectric power harvesting was verified. Besides that, it was also found that, by taking the ideal lossless case as reference, the relative counteractive effect against power harvesting becomes more significant under: 1) larger dielectric loss tangent, 2) weaker electromechanical coupling, 3) further away from resonance, 4) lower vibration frequency, and 5) with power-boosting interface circuit. Among these five factors, the first three are unwanted in efficient PEH systems. These three factors and their aggravations on counteractive effect should be simultaneously reduced through proper design. On the other hand, the fourth factor would be preferred in many practical scenarios for matching the spectrum of ambient vibration; the fifth factor is desired for further enhancing the power density of PEH systems [9]. For these two factors, trade off should be made between positive and counteractive effect in holistic design for practical PEH systems. In general, when the effect of dielectric loss cannot be ignored, additional concerns should be taken from material, structure, excitation, and circuit aspects towards accurate estimation on harvested power and design of practical PEH systems.

Acknowledgments

The work described in this paper was supported by ShanghaiTech University, Shanghai, China, under the Faculty Start-up Grant (Ref. No. F-0203-13-003), and the Research Grants Council of the Hong Kong Special Administrative Region, China, under Theme-based Research Scheme (Project No. T23-407/13-N).

References

[1] Anton S R and Sodano H A 2007 *Smart Mater. Struct.* **16** 1–21
[2] Tang L, Yang Y and Soh C K 2010 *J. Intell. Mater. Syst. Struct.* **21** 1867–97
[3] Szarka G D, Stark B H and Burrow S G 2012 *IEEE Trans. Power Electron.* **27** 803–15
[4] Ottman G K, Hofmann H F and Lesieutre G A 2003 *IEEE Trans. Power Electron.* **18** 696–703
[5] Erturk A and Inman D J 2008 *Smart Mater. Struct.* **17** 065016
[6] Liang J R and Liao W H 2011 *J. Intell. Mater. Syst. Struct.* **22** 503–12
[7] Hirose S, Aoyagi M and Tomikawa Y 1993 *Japan J. Appl. Phys.* **32** 2418–21
[8] Lallart M and Guyomar D 2010 *Appl. Phys. Lett.* **97** 014104
[9] Liang J R and Chung H S H 2013 *J. Phys. Conf. Ser.* **476** 012025
[10] Qiu J, Jiang H, Ji H and Zhu K 2009 *Front. Mech. Eng. Chin.* **4** 153–9
[11] Ji H, Qiu J, Badel A, Chen Y and Zhu K 2009 *J. Intell. Mater. Syst. Struct.* 939–47
[12] Ji H, Qiu J and Xia P 2011 *J. Sound Vib.* **330** 3539–60
[13] Kwok K W, Chan H L W and Choy C L 1997 *IEEE Trans. Ultrason. Ferroelectr. Frequation Control* **44** 733–42
[14] Yang Y and Tang L 2009 *J. Intell. Mater. Syst. Struct.* **20** 2223–35
[15] Shu Y C, Lien I C and Wu W J 2007 *Smart Mater. Struct.* **16** 2253–64
[16] Lien I C, Shu Y C, Wu W J, Shiu S M and Lin H C 2010 *Smart Mater. Struct.* **19** 125009
[17] Tang L and Yang Y 2011 *Smart Mater. Struct.* **20** 085022
[18] Liang J R and Liao W H 2012 *IEEE/ASME Trans. Mechatron.* **17** 1145–57
[19] Liang J R and Liao W H 2011 *Smart Mater. Struct.* **20** 015005
[20] Williams C B and Yates R B 1996 *Sensors Actuators* A **52** 8–11
[21] APC International, Ltd *Piezoelectric ceramics: principles and applications* www.americanpiezo.com/standard-products/textbook.html
[22] Smart Material Corporation *Piezo ceramic fiber and tubes flyer* www.smart-material.com/media/Datasheet/fibres-Version-2011.pdf
[23] Lefeuvre E, Badel A, Richard C, Petit L and Guyomar D 2006 *Sensors Actuators* A **126** 405–16